From “inverted” to “superdirect“ bonds: a general concept connecting substituent angles with sigma bond strengths. The case of the CC bonds in hydrocarbons.

Rubén Laplaza,[b] Julia Contreras-Garcia[c], Franck Fuster [c], François Volatron[c], and Patrick Chaquin*[a]

Abstract. The C-C bond energy with respect to geometry frozen fragments (BE) has been calculated for C_2H_6 as a function of θ = H-C-C angles. BE decreases rapidly when θ decreases from its equilibrium value to yield the so-called “inverted bonds” for $\theta < 90°$; on the contrary BE increases with θ to yield somehow “superdirect” bonds, following a sigmoidal variation related to orbital overlap. The central bonds in Si_2H_6, Ge_2H_6 and N_2H_4 as well as the C-H bond in CH_3-H behave similarly. The concept of “invertedness”/”directedness” is generalized to any CC σ bond in hydrocarbons and characterized by the mean angle value $<\theta>$ of substituents. Using dynamic orbital forces (DOF) as indices, the intrinsic σ bond energies are studied as a function of $<\theta>$ for 24 formally single bonds in a panel of 22 molecules. BE decreases from the strongest “superdirect” bonds in butadiyne, ($<\theta> = 180°$) or tetrahedrylacetylene to the weakest “inverted bonds” in cyclobutene, tetrahedrane, bicyclobutane and [1.1.1]propellane ($<\theta> = 60°$), following a sigmoidal variation. The $<\theta>$ parameter appears as a crude, but straightforward and robust, index of strain in cyclic molecules. In a panel of 11 formally multiple bonds, where typically $<\theta> < 90°$ σ contributions are found significantly weaker than standard single bonds. Thus they can be considered as formally inverted or near inverted.

Introduction

In a recent publication, we revisited the properties of the so-called “inverted bond” in [1.1.1]propellane (Figure 1).[1] Let us recall that inverted bonds result from the overlap of s+p hybrids by their smaller lobe (Figure 1), by contrast to “normal” or “direct” bonds in which overlap occurs between their bigger lobes. The energy of the central CC bond of propellane

[a] Pr. P. Chaquin
Laboratoire de Chimie Théorique (LCT)
Sorbonne Université, CNRS, F-75005 Paris
E-mail : chaquin@lct.jussieu.fr
[b] Dr. R. Laplaza
Laboratoire de Chimie Théorique (LCT)
Sorbonne Université, CNRS, F-75005 Paris

Departamento de Química Física
Universidad de Zaragoza
50009 Zaragoza, Spain
[c] Dr. J. Contreras-Garcia, Dr. F. Fuster, Dr. F. Volatron
Laboratoire de Chimie Théorique (LCT)
Sorbonne Université, CNRS, F-75005 Paris

was evaluated[2] to ca. 60 kcal/mol and this unexpected high value was the subject of many works.[3] Its origin was attributed either to a strong σ bond of "charge shift" nature[3b] or to π-type banana bonds ensured by the CH_2 bridges.[2c]

In ref 1., we used C_2H_6 models to mimic *in silico* the CC bond inversion by decreasing the θ = HCC angle from its optimized value, close to 111°, down to 70°. The CC dissociation energy, computed with respect to geometry frozen CH_3 moieties, was found to decrease rapidly and by extrapolation should tend to zero for HCC = 60°. The use Dynamic Orbital Forces (DOF) as indices of bond strengths confirmed this result: the intrinsic σ bond energy in propellane should be near zero, and thus the CC bonding is essentially π in nature. In a response by Braïda et al.,[4] this result was contested, arguing that, due to its charge shift nature, the bond strength in propellane could not be evaluated using DOFs.

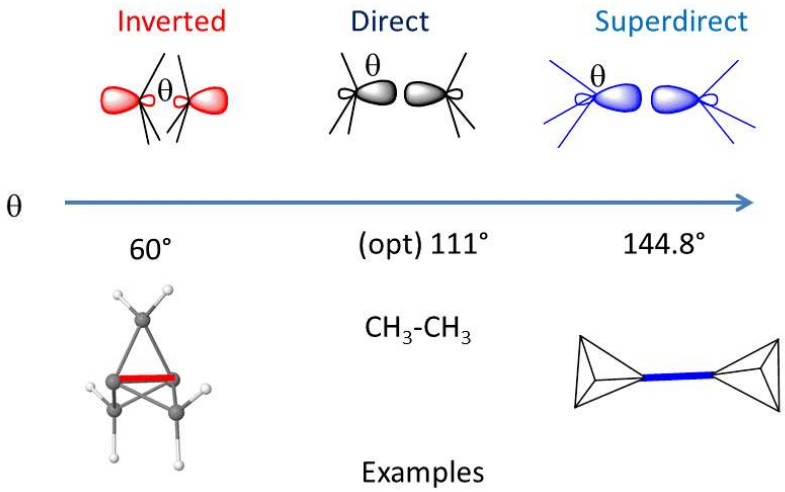

Figure 1. "Inverted", "direct" and "superdirect" bonds according to the θ angle of substituents. [1.1.1]Propellane, ethane and tetrahedryl-tetrahedrane exemplify these three types of bonds respectively.

By contrast, in some C-C bonds, the substituent angles are significantly greater than their value in ethane, with an associated increase of the bond energy. Though the unsubstituted molecule is unstable,[5] tetrahedryl-tetraedrane (Figure 1) is the limiting example of such a situation, with substituent angles close to 145° and a central bond remarkably strong (136 kcal/mol) and short (1.426 Å)[6] . We propose the term "superdirect" for such bonds. Thus, as displayed in Figure 1, sigma bonds can be classified into "inverted", "direct" and "superdirect" according to the value of the θ pyramidalization angle.

In the present work, our aim is to generalize the concept of invertedness vs. directedness to any sigma CC bond in hydrocarbons, in relation with its strength. In a first step C_2H_6 and related models will offer an *in silico* overview of this relation. Then we will characterize the degree of invertedness/directedness/superdirectedness by setting a "mean substituent angle" $<\theta>$ and we will consider the relation of this parameter with σ bond strengths in a panel of 35 bonds in 28 molecules. For this purpose, the Dynamic Orbital Forces (DOF) will be used as indices of intrinsic bond energy and as a tool of σ/π partition.

Computational Details

Optimized geometries and bonding energies with respect to geometry frozen fragments have been calculated at the CCSD(T)/cc-pVQZ level for C_2H_6 and CH_3-H models, and at the MP2/cc-pVTZ level for Si_2H_6, Ge_2H_6 and N_2H_4. The geometry of 28 hydrocarbon molecules was also optimized at the MP2/cc-pVTZ level. The derivatives of the canonical molecular orbitals were calculated, with the same basis set as geometry optimization, by a finite difference of bond lengths of 0.002 Å to 0.004 Å according to the case, thanks to a home-made script (available upon request). The Gaussian09 program was used throughout this work.[7]

Results and discussion

1. *In silico* C_2H_6 and related models

1.1. Influence of HCC angles on CC bond energy in C_2H_6

In the C_2H_6 model, all six θ = HCH angles are frozen from 70° to 145°. After optimization of the remaining geometrical parameters, the C-C bond energy (BE) with respect to geometry frozen CH_3 moieties has been computed at the CCSD(T)/cc-pVQZ level. In this model (Table 1 and Figure 2), BE decreases rapidly when θ decreases from the optimized geometry to yield an inverted bond; it increases significantly with θ to yield a superdirect bond.

Table 1. The C_2H_6 model. Geometrical parameters R(Å) and bonding energy BE (kcal/mol, with respect to two CH_3 at frozen geometry) as function of θ (CCSD(T)/cc-pvQZ). The results for θ ≤ 111.2° are taken from ref. 1.

	C_2H_6									
θ	145°	140°	130°	120°	opt (111.2°)	100°	95°	90°	80°	70°
R(CC)	1.411	1.422	1.448	1.483	1.527	1.628	1.708	1.830	2.231	2.9
R(CH)	1.18	1.135	1.111	1.097	1.091	1.085	1.082	1.079	1.079	1.089
BE	154.2	152.8	145.0	131.6	114.1	81.6	63.3	44.5	15.4	5.6

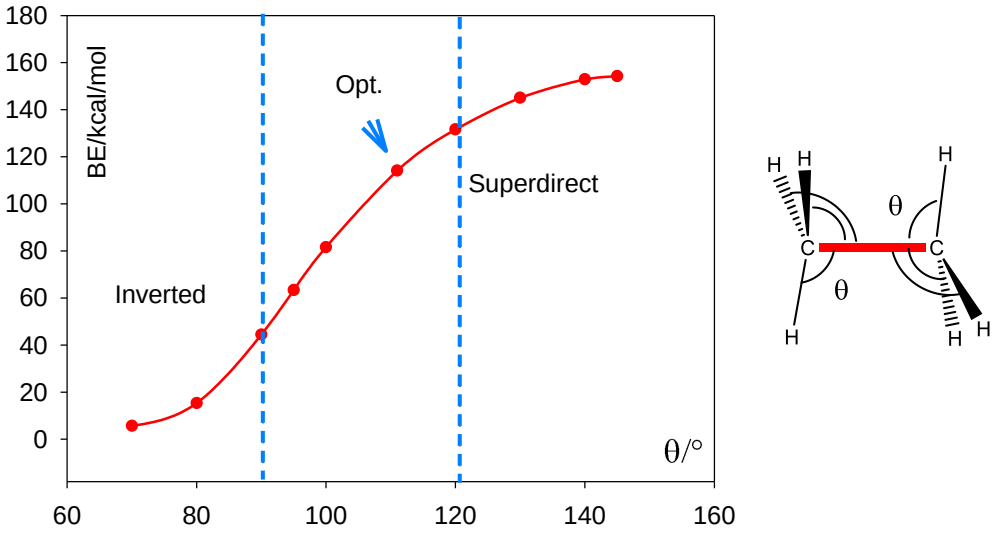

Figure 2. CC bond energy (BE) in C_2H_6 with respect to geometry frozen CH_3 fragments as a function of θ = HCC angles (θ = 111.2° optimized value); CCSD(T)/cc-pvQZ.

1.2. Qualitative interpretation

The overall sigmoidal shape of BE curve as a function of θ can be interpreted qualitatively by an evaluation of the overlap of both s+p hybrids, h_1 and h_2 (Figure 3).

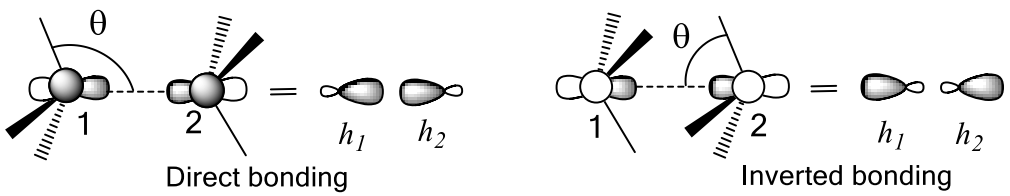

Figure 3. Overlap in direct and inverted bonding.

The hybrids h_1 and h_2 are written as:

$$h_1 = \alpha s_1 + \beta p_1$$
$$h_2 = \alpha s_2 + \beta p_2$$

with $\alpha^2 + \beta^2 = 1$. Setting $\beta > 0$:

$\alpha < 0$ for $\theta < 90°$

$\alpha = 0$ for $\theta = 90°$

$\alpha > 0$ for $\theta > 90°$

The theoretical limits of θ are 0°, with $\alpha = -\beta = -1/\sqrt{2}$ and 180°, with $\alpha = \beta = 1/\sqrt{2}$. The corresponding hybridization states can be referred to as sp^{-1} and sp respectively. Between these limits, the following hybridization states are encountered: sp^{-2} ($\alpha = -1/\sqrt{3}$), sp^{-3} ($\alpha = -1/2$), s^0p ($\alpha = 0$), sp^3 ($\alpha = 1/2$), sp^2 ($\alpha = 1/\sqrt{3}$). The following values of α for CH_3 are obtained with the minimal basis STO-3G for CH_3 and various θ (Table 2). The limit between sp^3 and sp^2 occurs at θ = 120° which can be taken as the (arbitrary) limit between "direct" and "superdirect" bonds.

Table 2. Coefficient α of the s AO in the CH_3 SOMO hybrid as a function of θ angle (see Figure 3).

θ	60	70	80	90	100	110	120	130	140
α	-0.601	-0.483	-0.294	0.000	0.294	0.483	0.601	0.693	0.786

The overlap *S* of h_1 and h_2 is given by:

$$S = \langle \alpha s_1 + \beta p_1 | \alpha s_2 + \beta p_2 \rangle = \alpha^2 \langle s_1 | s_2 \rangle + \beta^2 \langle p_1 | p_2 \rangle + 2\alpha\beta \langle s_1 | p_2 \rangle \qquad (1)$$

In a first step, the overlaps S_e of s+p hybrids of CH_3 have been computed at the CC equilibrium distances in the C_2H_6 model for each θ value (red curve in Figure 4a). Then, in order to emphasize the effect of hybridization alone, the overlap S_0 has been determined for a constant CC distance of 1.5 Å. Note that, in this case, to a first approximation, the three atomic overlaps in Eq. 1 are close to 0.3:

$$S_0 \approx 0.3(\alpha^2 + \beta^2 + 2\alpha\beta) = 0.3(1 + 2\alpha\beta) \qquad (2)$$

The corresponding values are reported in Figure 4a (black curve). Both S_0 and S_{eq} as a function of θ have a sigmoidal shape similar the bonding energy in Figure 2. The two curves are nearly coincident for θ < 110° indicating the prominent role of the hybridization in this region. Moreover, the bonding energy appears closely connected to both S_{eq} *and* S_0 (Figure 4 (b)), with, again a quasi-superimposition in the corresponding region.

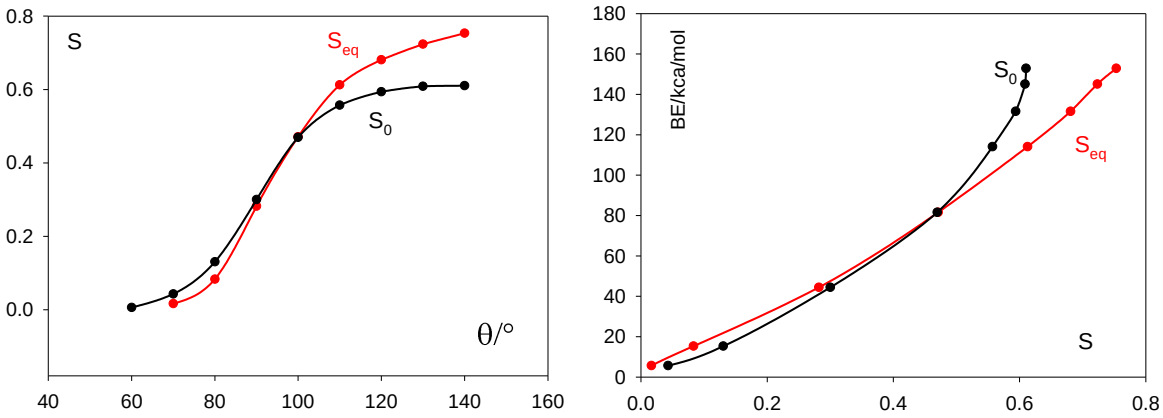

(a) (b)

Figure 4. (a) Variation of overlap S with θ in C_2H_6 model: S_{eq} at equilibrium R(CC) distance (red curve); S_0 for a CC constant distance of 1.5 Å (black curve). (b) Variation of CC bond energy BE as a function of S_{eq} (red curve) and S_0 (black curve).

1.3. Related models: Si_2H_6, Ge_2H_6, N_2H_4 and CH_4

Though we are mainly interested in CC bonds in this work, we examined some models involving other bonds to compare their behaviour when similar angle constraints are imposed.

Two heavier systems, Si_2H_6 and Ge_2H_6, have been studied at the MP2/cc-pVTZ level following the approach of the C_2H_6 model. Figures 5(a) and 5(b) display the variation of BE as a function of the θ angles H-Si-Si and H-Ge-Ge respectively. The two curves are very similar. They have also the same general shape as for C_2H_6, with a weaker BE increase in the superdirect region (θ > 120°). It appears that the decrease of the ns-np gap in these both species, with respect to C_2H_6, is only of minor consequence as compared to the angle variation.

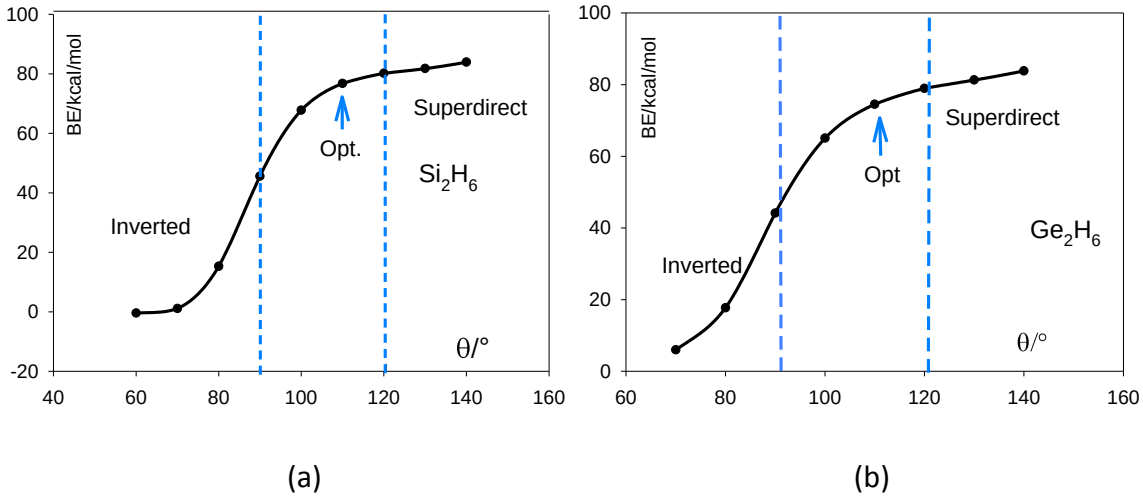

Figure 5. Central bond energies of Si_2H_6 (a) and Ge_2H_6 (b) as functions of θ angles (H-Si-Si and H-Ge-Ge respectively).

The BE of the NN bond of NH_2-NH_2 in D_{2d} symmetry was also studied as a function of θ = HNN angles. The dissociation energy was computed with respect to geometry frozen NH_2 fragments in their $^2A_1$ state. It should be noted that N-N bond breaking results in the formation of two NH_2 radicals possessing a lone pair in a 2p AO and a semi occupied s+p hybrid. In its optimized geometry, this state is ca. 34 kcal/mol above the $^2B_1$ ground state.[8] Thus the value of BE in geometry optimized N_2H_4 lies at 68 kcal/mol above the NN dissociation energy into $2NH_2$ in their ground state.

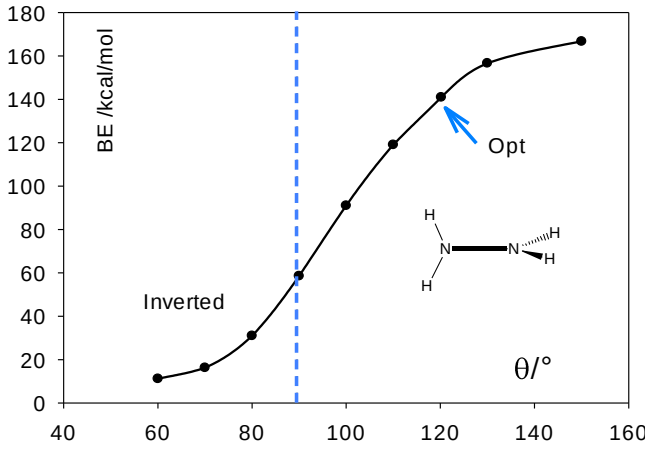

Figure 6. N-N bond energy in N_2H_4 (D_{2d}) as a function of θ = H-N-N angles.

Finally, we studied the energy of one C-H bond in CH_4 as a function of the θ pyramidalization angle of the CH_3 moiety. Results in Table 3 and Figure 6 are similar to the preceding ones. Nevertheless, because we deal here with the deformation of only one CH_3 group, yielding either "semi-inverted" or "semi superdirect" bonds, the relative variation of BE is smaller than in the case of C_2H_6 (cf. Figure 2).

Table 3. H_3C-H. Geometrical parameters R (Å) and bond energy BE of CH (kcal/mol, with respect to H and CH_3 at frozen geometry) as function of θ; opt = 109.5°; CH1 refers to H in CH_3 group; CCSD(T)/cc-pVQZ level of calculation.

	H_3C-H								
θ	140°	130°	120°	opt	100°	90°	80°	70°	60°
R(CH)	1.063	1.068	1.076	1.087	1.105	1.132	1.174	1.229	1.290
R(CH1)	1.134	1.108	1.095	1.087	1.085	1.084	0.876	1.003	1.130
BE	138.4	134.1	127.7	119.4	107.5	90.6	70.8	54.1	44.9

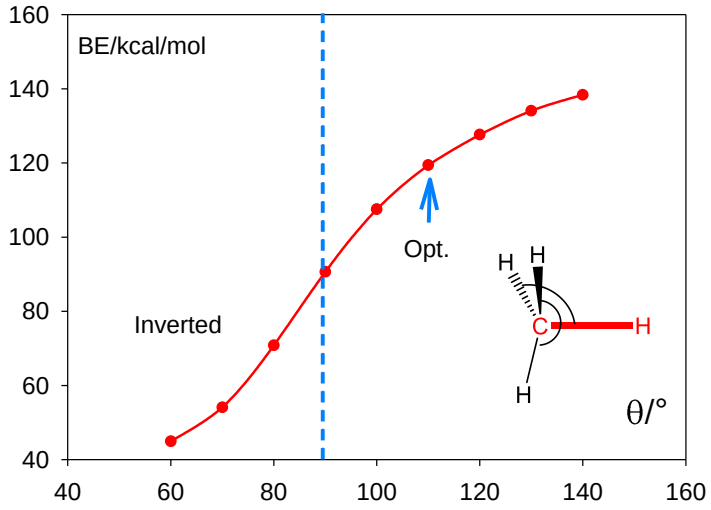

Figure 7. CH bond energy in H_3C-H (red bond) as a function of θ = HCH angle.

All studied models agree with the fact that the bond energy is strongly dependent on the substituent angles: it decreases rapidly with the inverted character of the bond and increases with its superdirect character. These phenomena follow the variation of the hybridization of the s+p AOs overlapping in the bond formation, controlled by these angles. Specifically, BE increases with the s (algebraic) coefficient in the s+p hybrids. This result is well-known for "direct" C-H bonds with aliphatic (sp^3), ethylenic (sp^2) and acetylenic (sp)

carbons[9]. It has been also pointed out with direct C-C bonds[10], for example regarding the strong central bond of tetrahedryl-tetraedrane.[6b,11] Nevertheless, the final optimized CC distance involves other parameters as evidenced by energy decomposition analysis.[12] Moreover, it was shown in a recent work that the contraction of CC bonds along a series $C(sp^3)$-$C(sp^3)$, $C(sp^3)$-$C(sp^2)$ and $C(sp^3)$-C(sp) does not originate from an increase in the s character of the second atom, but in a decrease of the steric (Fermi) repulsion between substituents of both carbons.[13] Indeed, in the AH_n-AH_n models of the preceding study, we observe that direct bonds shorten as θ increases, together with H…H distances resulting in weaker Fermi repulsion. The situation is less clear for inverted bonds. As an example, in C_2H_6, for θ = 90° R(CC) = 1.830 Å with H…H = 2.12 Å. For θ = 80° the H…H distance increases very weakly (2.14 Å), resulting in a negligible decrease in Fermi repulsion, while R(CC) significantly increases by 0.4 Å (2.231 Å). It suggests that the bond length could be controlled by hybridization in inverted bonds.

2. Inverted, direct, and superdirect bonds: generalization for sigma CC bonds in hydrocarbons

2.1. Mean angle <θ> of substitution

The preceding models preserve a symmetry axis along the bond under scrutiny with equal angles of H substituents on each heavy atom (pyramidalization angle). We will now extend the inverted/direct/superdirect character to any CC σ bond in hydrocarbons, be it formally a single bond or a σ bond in a formally multiple bond. For this purpose, we define a <θ> parameter as simply the mean value of the angles of the six substituents on both carbon atoms; the π bonds are treated as σ ones in these calculations. Two examples are given in Figure 8.

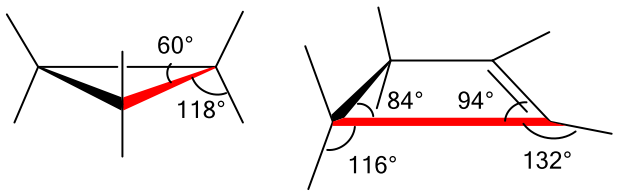

Figure 8. Calculation of the <θ> angle for the red bond in cyclopropane and cyclobutene.

In cyclopropane, the red bond has 4 H at 118° and two C at 60°, yielding <θ>≈ 99°. In cyclobutene, the red bond is considered as having 2 C at 94°, 1 H at 132°, 1 C at 84° and 2H at 116.° yielding <θ> = 106°. This way, the central C-C bond in butadiyne HC≡C—C≡CH has the <θ> theoretical maximum value of 180°. In formally multiple bonds, the <θ> angle is determined in a similar way. For example, in acetylene H-C≡C-H, the σ CC bond in considered as having 4 C at 0° and 2 H at 180°, yielding <θ> = 60°.

2.2. Dynamic orbital forces as index of intrinsic bond energy and tool for σ/π partition

For the study of the relation between σ bond strength and <θ> in real systems, 35 CC bonds of various <θ> were considered in a panel of 28 molecules (Tables 4 and 5). In many of these cases, the BE of C-C bonds can no longer be computed in the same way as in the first section. Thus we will use the dynamic orbital forces (DOF)[14] as indices of bond energies.

The derivative of the i^{th} canonical MO energy ε_i with respect to a bond length (R(CC) in the case of a CC bond) has already been used to characterize the bonding/antibonding character of the MO with respect to this bond.[15] Also it has been shown that a MO of positive DOF has a positive contribution to the dissociation energy.[16] The sum Σ_{tot} of these derivatives over valence occupied MOs by n_i electrons can be decomposed into σ (Σ_σ) and π (Σ_π) components:

$$\Sigma_{tot} = \sum_i^{occ} n_i \frac{d\varepsilon_i}{dR(CC)} = \sum_j^{\sigma occ} n_j \frac{d\varepsilon_j}{dR(CC)} + \sum_k^{\pi occ} n_k \frac{d\varepsilon_k}{dR(CC)} = \Sigma_\sigma + \Sigma_\pi$$

It has been recognized that Σ_{tot} is an index of the "bond strength", as far as the molecule is satisfactorily described at the Hartree-Fock (H-F) level.[17,18] However Σ_{tot} is an intrinsic quantity of the system, whereas the bond energy dissociations with respect to geometry frozen fragments (BE) considered in the preceding sections involve the electronic relaxation of fragments and thus some reorganization energy. This tends to lower BE with respect to the intrinsic bond energy, but this difference should be small if the two following conditions are fulfilled: (i) the bond is symmetrically or nearly symmetrically substituted, resulting in a negligible electron transfer by bond dissociation and (ii) no significant stabilization of the radicals obtained occurs by conjugation or hyperconjugation. In Figure 9, we report Σ_{tot} for the C_2H_6 model and various CC bonds (taken from ref. 17). We observe an excellent linear

correlation (R^2 = 0.98) of BE of CC bonds and Σ_{tot} in the series C_2H_2, C_2H_4, C_6H_6, C_2H_6 and C_3H_6 (black line in Figure 9). Regarding the C_2H_6 model with various θ values (red curve in Figure 9), the curve is strictly superimposed to the preceding black line for $\Sigma_{tot} > 0.4$. For smaller Σ_{tot} values, the slope decreases and BE tends to zero for $\Sigma_{tot} \approx 0$.

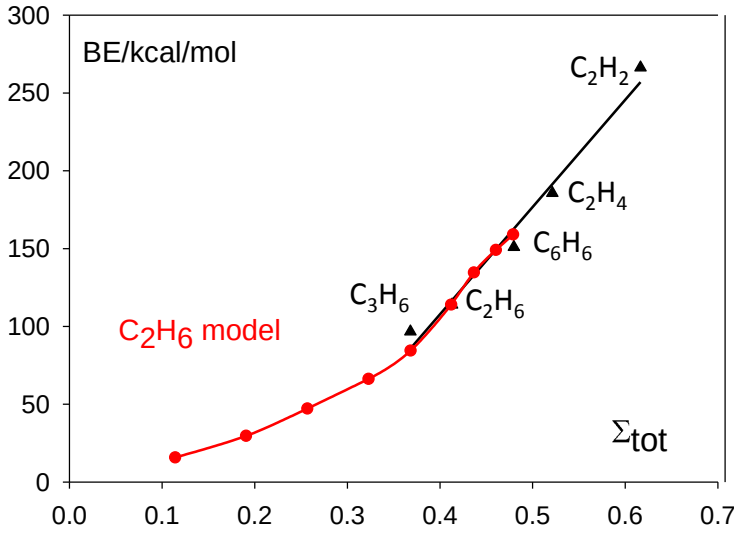

Figure 9. Bond energy (kcal/mol) with respect to geometry frozen fragments (MP2/cc-pVTZ) as a function of Σ_{tot} (a.u.).

This way, Σ_{tot}, though computed from H-F level MOs, is found to be correlated to CC bond strength. This empirical observation is further supported by a large amount of evidence regarding bond energies. Indeed, a very good correlation (R^2 = 0.97) is found with respect to BE values calculated at the DFT ωB97XD/aug-qzvp level for bonds **1, 12**, **19**, **27, 26, 29, 34** of Tables 4 and 5.[19] Moreover, Σ_{tot} can be compared with intrinsic bond energies computed from AIM critical point properties and bond paths (using, of course, correlated electron densities).[10,20] A rather good linear correlation is again obtained (R^2 = 0.94) with the set of bonds **1**, **4**, **8**, **9**, **12**, **13**, **18**, **19**, **26**, **29**, **30**, **33, 34** of Tables 4 and 5. Thus, as far as the molecule is satisfactorily described at the H-F level, we consider Σ_{tot} as a straightforward empirical index (even predictive) allowing the comparison of the CC intrinsic bond strengths in hydrocarbons. Moreover, Σ_σ and Σ_π reflect their relative σ and π components.

2.3. Sigma CC bond energy and mean angle of substitution <θ>

2.3.1. Formally single bonds

In Table 4, we report the values of Σ_{tot}, Σ_{σ} and Σ_{π} in a panel of formally single 24 C-C bonds, displayed in Figure 10, by order of decreasing values of <θ> from 180° to 60°. The concept of directedness/invertedness concerns σ bonds, and thus we will be interested mainly in the Σ_{σ} component, though Σ_{tot} and Σ_{π} could also offer useful information.

Table 4. Values of Σ_{tot} , Σ_{σ}, Σ_{π} (a.u.); % of Σ_{π} in Σ_{tot} , equilibrium bond length R(CC) (Å) and the corresponding values of <θ> (°) for formally single C-C bonds (TET = tetrahedryl; BCP = bicyclopentyl; CUB = cubyl, see also Figure 10).

Label	Molecule	Σ_{tot}	Σ_{σ}	Σ_{π}	% π	R(CC)	<θ>
1	HC≡C—C≡CH	0.513	0.450	0.064	12.4	1.369	180
2	TET—C≡CH	0.527	0.437	0.090	17.1	1.394	163
3	TET—TET	0.468	0.447	0.021	4.5	1.419	145
4	CH_3—C≡CH	0.458	0.415	0.042	9.1	1.458	145
5	TET—CH_3	0.495	0.442	0.053	10.1	1.476	128
6	BCP—BCP	0.489	0.434	0.055	11.3	1.477	127
7	CUB—CUB	0.478	0.420	0.058	12.1	1.465	125
8	CH_2=CH—CH=CH_2	0.478	0.433	0.045	9.4	1.453	121
9	CH_3—CH=CH_2	0.418	0.399	0.019	4.5	1.505	116
10	Ph—CH_3	0.415	0.397	0.019	4.6	1.503	115
11	$(CH_3)_3C$—$C(CH_3)_3$	0.439	0.392	0.048	10.8	1.565	111
12	CH_3—CH_3	0.413	0.392	0.021	4.9	1.527	111
13	cyclohexane	0.445	0.425[a]	0.02[a]	4.5[a]	1.565	110
14	methenecyclopropane (3-4)	0.414	0.397	0.017	4.1	1.464	109
15	cyclopentane	0.420	0.403	0.017[b]	4.3	1.526	108
16	cyclobutene (2-3)	0.445	0.400	0.045	10.1	1.537	106
17	cyclobutene (3-4)	0.404	0.396	0.008	2.0	1.565	105
18	cyclobutane	0.408	0.401	0.007[b]	1.7	1.546	105
19	cyclopropane	0.364	0.368	-0.004	-1.1	1.504	99
20	methenecyclopropane (1-2)	0.333	0.333	0.000	0.0	1.539	97
21	cyclopropene	0.281	0.283	-0.002	-2.0	1.508	88
22	tetrahedrane	0.353	0.278	0.075	21.2	1.478	88
23	bicyclobutane	0.360	0.215	0.146	39.7	1.500	82
24	[1.1.1]Propellane	0.275	-0.029	0.304	110.5	1.596	60

[a] Estimated on the basis of the same Σ_{π} =0.02 a.u. as **12**. [b] The π MOs have been visually identified, which can lead to some uncertainty.

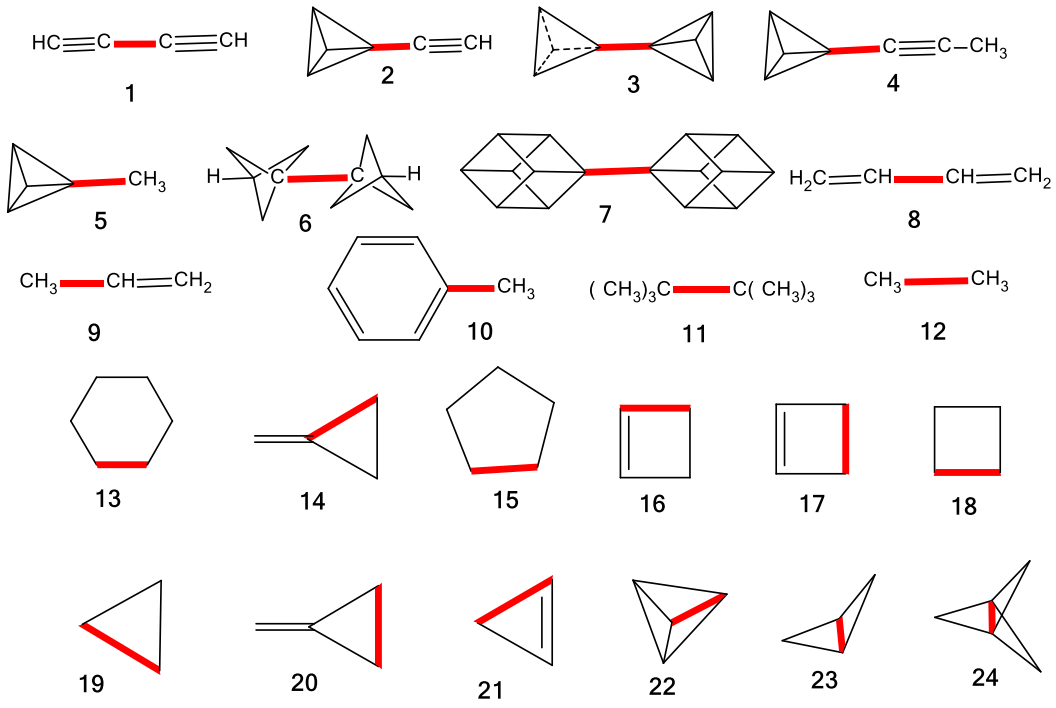

Figure 10. Bonds and molecules of Table 5.

Molecules **1**-**8** can be considered as having a superdirect bond, with Σ_σ ranging from 0.415 up to 0.450 a.u. for butadiyne **1,** which has the maximum theoretical value of <θ> (180°). For the direct bonds **9**-**18 (**116° **<** <θ> < 105°) **,** Σ_σ is generally close to 0.4 a.u. Ethane **12** can be taken as the prototype of "standard" direct CC bond with Σ_σ = 0.392 a.u. Bonds **19** and **20**, are formally direct (<θ> = 99° and 97° respectively) but have significantly lower Σ_σ (0.368 and 0.333 a.u. respectively) according to ring strain. Molecules **21**-**24** possess inverted bonds and Σ_σ less than 0.283 a.u., corresponding to strong strains, down to a slightly negative value in propellane **24** (-0.029 a.u. with <θ> = 60°).

We thus observe (Figure 11) a general increase of Σ_σ with <θ>, following the same sigmoidal shape as observed for the models of sections 1 and 3. As a landmark, we report on the same figure the variation of Σ_σ for the C_2H_6 model (red curve), showing that the behaviour of real bonds is quite similar to that of this C_2H_6 model.

The value of Σ_{tot} in tetramethylbutane **11** (0.439 a.u.) suggests that its intrinsic bond energy is greater than that of ethane **12** (0.413 a.u.) though its experimental dissociation energy is significantly smaller (78.6 kcal/mol vs. 90.2 kcal/mol).[21] Nevertheless, the BE of both species

with respect to geometry frozen fragments (MP2/cc-PVTZ) are found nearly equal (113.0 kcal/mol for **11** and 113.9 for **12**). Moreover, the electronic relaxation in $Me_3C^{\cdot}$ radical involves a significant stabilization by hyperconjugation, which leads to an underestimation of the calculated BE of **12** with respect to the actual intrinsic value.

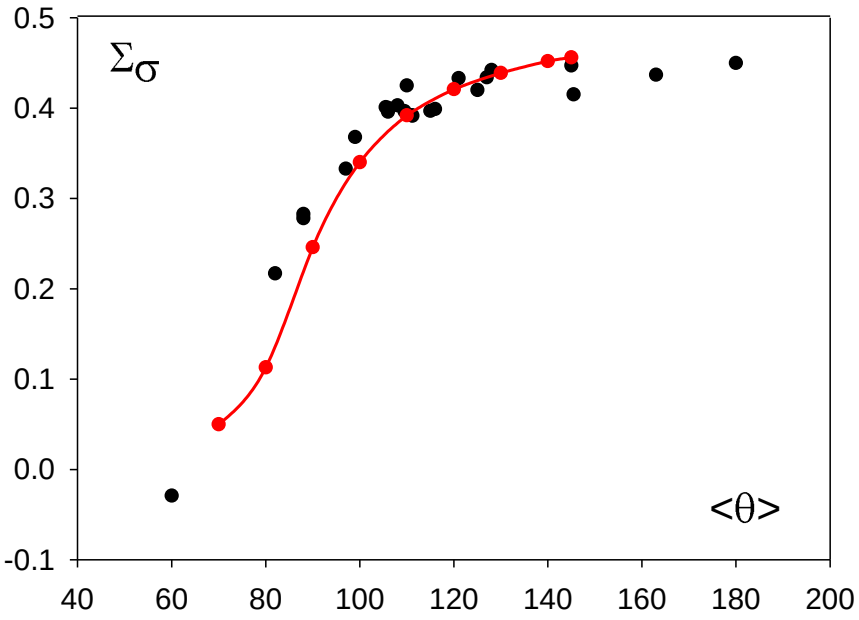

Figure 11. Σ_σ (a.u.) values for bonds in molecules **1**-**22** with respect to the mean substituent angle <θ> (°). The red curve corresponds to C_2H_6 model.

The π participation to Σ_{tot}, corresponding to the total bond strength, is generally no more than ca. 10 % in all superdirect or direct bonds. In can be noted that the high BE in butadiyne **1** as compared to that of ethane **12** is due to σ strengthening ($\Delta\Sigma_\sigma$ = 0.058 a.u.) more than to conjugation ($\Delta\Sigma_\pi$ = 0.043 a.u.). The same remark holds for butadiene **8**, whose corresponding values are $\Delta\Sigma_\sigma$ = 0.041 a.u. and $\Delta\Sigma_\pi$ = 0.024 a.u. Also, it has been proposed that the strong bond of **3** originates equally both from its high s character and from hyperconjugation;[22] but in the present work the hyperconjugation term appears weak, with only 4.5 % contribution of π MOs to Σ_{tot}. This is further supported by the 12% of π energy that was determined from Energy Decomposition Analysis.[6b]

In the series of cyclanes, we observe a regular decrease of Σ_{tot}, as the ring strain increases: cyclohexane **13** (0.445 a.u.), cyclopentane **15** (0.420 a.u.), cyclobutane **18** (0.408 a.u.) and cyclopropane **19** (0.368 a.u.). Because their rings are non-planar (except cyclopropane **19**),

the π MOs have been identified visually for **15** and **18**. For cyclohexane **13** the σ/π partition becomes problematic because most of the MOs have both types of participation; we assumed that Σ_π is close to the value observed for ethane. Under these conditions, a decrease of Σ_σ is also observed along the series together with <θ>. The slightly negative π participation in **19** and **21** can be due to their quasi-eclipsed conformation, this participation being nearly zero in eclipsed ethane. Furthermore, it is well known that cyclobutane **18** and cyclopropane **19** have very close strain energies, 26.5 kcal/mol and 27.5 kcal/mol respectively[23], though the three-membered cycle could appears as much more strained. Taking into account that these energies involve all the bonds, it has been suggested that three weaker CC bonds in cyclopropane are compensated by six stronger CH bonds.[24] Indeed, <θ>(CH) = 109.5° for **18** and 116.3° for **19**: thus the CH bonds in cyclopropane are found to have some superdirect character. Moreover, from Table 3, the C-H BE increase can be evaluated to ca. 6.9 kcal/mol, close to previous determinations (8.6-8.8 kcal/mol).[25]

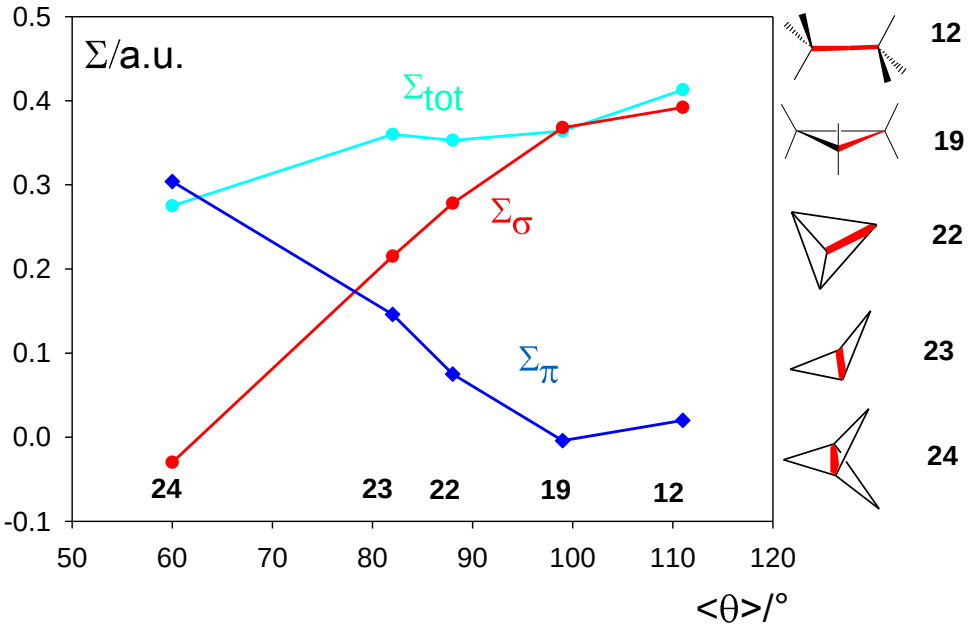

Figure 12. Various Σ values (a.u.) for CC bonds in ethane and a series of three-membered cyclic molecules (red bond).

The series of three-membered ring species **19**, **22**, **23** and **24**, compared to ethane **12** (Figure 12), is of a particular interest. The CC bond undergoes a progressive inversion with <θ> decreasing from 111.2° (direct bond in **12**) to 60° (inverted bond in propellane **24**). Σ_σ

decreases monotonously from 0.392 a.u. in ethane down to -0.029 a.u. in propellane. But at the same time, this decrease is compensated to a large extent by an increase of Σ_π for **22**, **23** and **24**. As a matter of fact, the presence of two CH bridges in **22**, two and three CH_2 bridges in **23** and **24** respectively, allows the formation of "banana bonds" of π character. The relative contributions of MOs to σ and π bonding have been detailed in ref. 1 in the case of propellane **24**. The "banana bonds" of bicyclobutane **23** are displayed in Figure 13. They are characterized, according to their π nature, by a nodal plane containing the central bond and are of a_2 and b_2 symmetry within the C_{2v} group. One of these MOs (14) is found antibonding (DOF = -0.069 a.u.) while the other three are bonding.

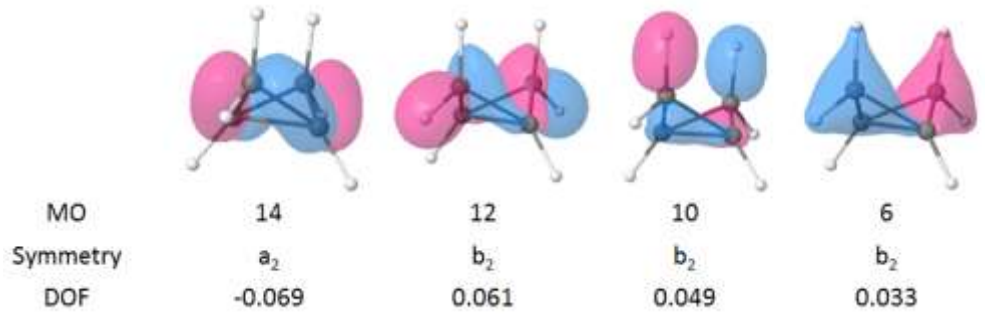

Figure 13. Bridge ("banana") bonds, and corresponding DOF (a.u.) of bicyclobutane **23**.

It is worthy to insist on the fact that, on the basis of the evolution of the Σ and $\langle\theta\rangle$ values, the central bond of propellane **24** behaves as expected in this series and does not appear as a particular case, in spite of its "charge shift" character within VB method.

The variation of R(CC) as a function of $\langle\theta\rangle$ deserves a comment. Bonds **1-13** have a generally weak π participation and they are not subject to cycle constraints. Their lengths thus result from a free interplay of their strength (essentially controlled by their s component) and the Fermi repulsion of their substituents: both these parameters tend to shorten the CC bond as $\langle\theta\rangle$ increases, as observed in Figure 14 (blue squares). These bonds have the same characteristics as the CC bond in the C_2H_6 model which behaves similarly (red curve). By contrast, bonds **14**-**24** are subject to cycle constraints and π component of various importance, and their bond lengths (cyan circles) diverge from those of the C_2H_6 model.

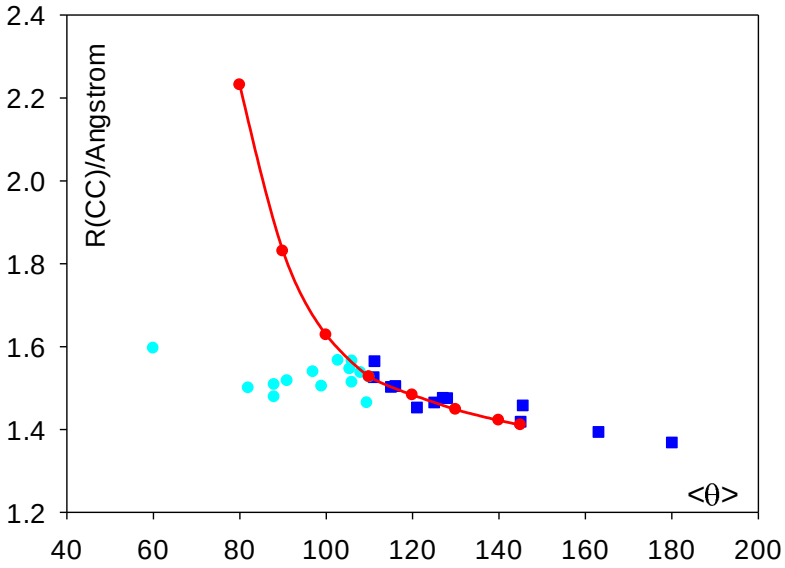

Figure 14. Bond lengths (Å) vs. mean angle <θ>; bonds **1**-**12** (blue squares); bonds **12**-**24** (cyan circles); C_2H6 model (red curve).

2.3.2. Sigma bonds in formally multiple bonds

From a panel of 11 formally multiple bonds, displayed in Figure 15, we report in Table 7 the values of Σ_{tot} , Σ_{σ}, Σ_{π} (a.u.) and the mean angle <θ> calculated for their σ component. For benzene **24**, <θ> = 100° is the mean of the two values of Kékulé structures.

The Σ_{tot} values range from 0.479 a.u. to 0.579 a.u. for double bonds, from 0.577 a.u. to 0.616 a.u. for triple bonds and is 0.480 a.u. for the "half double bond" of benzene. As expected, Σ_{tot} is slightly smaller in the conjugated **30** and **33** than in the corresponding non conjugated **29** and **34**.

Table 6. Values of Σ_{tot}, Σ_{σ}, Σ_{π} (a.u.) for CC bonds in multiple bonds and the corresponding values of $\langle\theta\rangle$ (°) for their σ bond (=C_3H_4 : cyclopropylidene, cf. Fig. 15).

label	Molecule	Σ_{tot}	Σ_{σ}	Σ_{π}	% π	R(CC)	$\langle\theta\rangle$
25	$H_2C{=}C{=}CH_2$	0.516	0.315	0.201	39.0	1.308	100
26	C_6H_6	0.480	0.342	0.139	29.9	1.394	100[a]
27	$H_4C_3{=}C_3H_4$	0.537	0.354	0.183	34.0	1.316	97
28	$CH_2{=}C_3H_4$	0.479	0.265	0.214	40.9	1.323	90
29	$H_2C{=}CH_2$	0.521	0.267	0.254	48.8	1.332	81
30	$CH_2{=}CH{-}CH{=}CH_2$	0.488	0.256	0.232	52.6	1.340	80
31	cyclobutene	0.519	0.283	0.236	45.5	1.350	77
32	cyclopropene	0.579	0.277	0.304	52.5	1.300	71.5
33	$HC{\equiv}C{-}C{\equiv}CH$	0.577	0.159	0.418	72.4	1.219	60
34	$HC{\equiv}CH$	0.616	0.145	0.471	76.5	1.211	60
35	cyclopentyne	0.524	0.087	0.437	83	1.245	40

[a] Mean value of the two Kékulé structures.

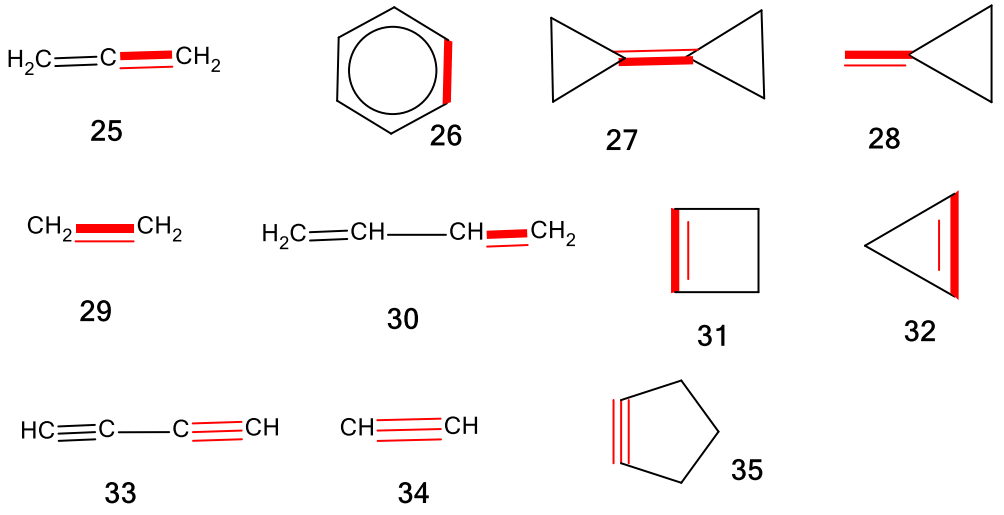

Figure 15. Bonds and molecules of Table 6.

The $\langle\theta\rangle$ values corresponding to the σ part of the double and triple bonds are greater than 90° only in **25**, **26** and **27.** Indeed, their Σ_{σ} values are smaller than that of cyclopropane **19** (0.372 a.u.). The σ participation to Σ_{tot} is generally close to 50% in standard alkenes and no

more than ca. 25% in alkynes, which has been already noted.[17] Their variations as a function of <θ> are shown in Figure 16 with the same scale as in Figure 11 for the sake of comparison. Like in formally single bonds, Σ_σ tends to decrease with <θ>, but significantly more slowly. From these results, the σ bond in multiple bonds can be generally considered as formally inverted.

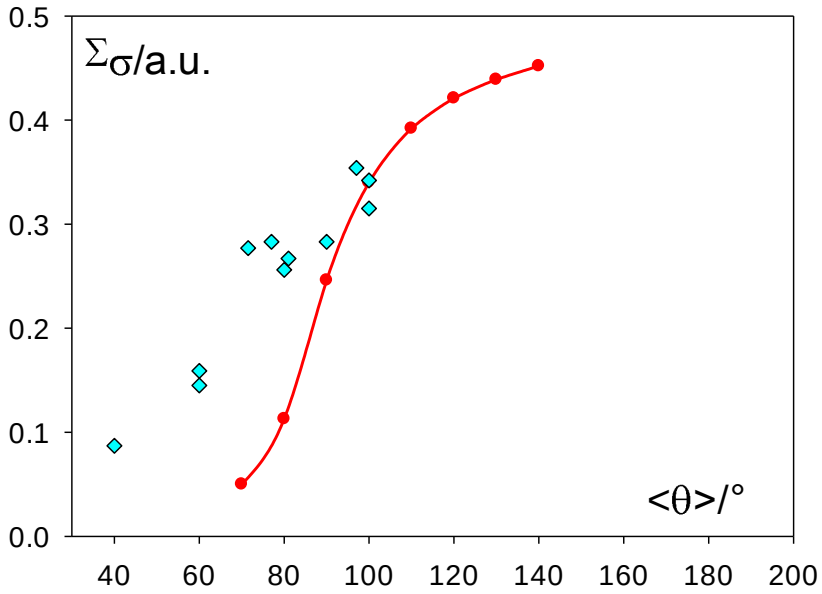

Figure 16. Values of Σ_σ (a.u.) for the σ bond in the formally multiple bond compounds **22**-**33** (cyan diamonds). The red curve corresponds to the C_2H_6 model for comparison.

The series **26**, **27** and **28** is illustrative of the influence of bond angles on σ bonds in double bonds (Table 7). The presence of two cyclopropenyl fragments in **27** tends to increase <θ> and Σ_σ, with respect to **28** and **27**. The same evolution is observed from cyclobutene **31** to cyclopropene **32**.

The σ bonds of alkynes possess formally four C substituents at 0° and thus have a maximum <θ> value of 60°. Because cyclopropyne and cyclobutyne are unstable, cyclopentyne **35** appears to possess a σ bond with the smallest possible <θ> value (40°) and thus the weakest Σ_σ (0.087 a.u.) among all multiple bonds considered. In turn, the small <θ> value for σ in triple bonds entails for <θ>(CH) its maximum theoretical value of 180° in **33** and **34**, in agreement with high CH bond dissociation in acetylene and hydrogen cyanide.

Conclusion

The bonding energy BE of the CC bond in the CH_3 -CH_3 model is strongly dependant of the θ = HCH angle, exhibiting a sigmoidal variation. Starting from θ equilibrium value, BE decreases rapidly when θ decreases to yield "inverted bonds" (θ < 90°) and tends to zero for θ = 60°-70°. On the contrary, BE increases when θ increases above its equilibrium value. We propose the term "superdirect" for the latter type of bonds. Within MO framework, this general behaviour is closely related to the s participation in the s+p hybrid AOs.

These results can be generalized to any CC sigma bond in hydrocarbons by defining a parameter <θ> as the mean value of its substituent angles. Using the sum of dynamic orbital forces (DOF) as index of intrinsic bond energy, the σ strength in formally single CC bonds increases according to a sigmoidal variation as function of <θ> (from a panel of 24 bonds in 22 molecules). The <θ> parameter thus appears as a crude, but straightforward and robust, index of the strain exerted on a σ bond: this strain can be "negative" which weakens the bond as its "inverted" character increases, or it can be "positive", resulting in a strengthening of the bond as its "superdirect" character increases. It accounts, among others, for the strain energy of cyclanes. It is also shown that in the series cyclopropane, bicyclobutane, tetraedrane and propellane, the strength of the σ bond common to 3-membered rings decreases with <θ> with respect to cyclopropane (<θ> = 99°) to vanish in propellane (<θ> = 60°). At the opposite, the strongest σ CC bonds are found in butadiyne (<θ> = 180°) and bonds having tetrahedryl and/or ethynyl substituent(s) (<θ> >120°). The method is also applied to σ bonds in formally multiple bonds, with a panel of 11 molecules. These systems correspond to small <θ> values and σ bonds significantly weaker than in standard single bonds. This way, σ bonds in multiple bonds can be considered as formally inverted in most of cases.

[1] R. Laplaza, J. Contreras-Garcia, F. Fuster , F. Volatron, P. Chaquin, *Chem. Eur. J*. **2020**, *26*, 6839-6845.

[2] a) K. B. Wiberg, F. H. Walker, *J. Am. Ckem. Soc.* **1982,** *104,* 5239-5240; b) D. Feller, E. R. Davidson, *J. Am. Chem. Soc.* **1987***, 109,* 4133-4139; c) J. E. Jackson, L. C. Allen, *J. Am. Chem. Soc* **1984**, *106*, 591-599.

[3] a) T. Kar, K. Jug, *Chem. Phys. Lett*. **1996**, *256*, 201-206; b) W. Wu, J. Gu, J. Song, S. Shaik, P. C. Hiberty *Angew. Chem*. **2009**, *121*, 1435 –1438; c) M. D. Newton, J. M. Schulman, *J. Am. Chem. Soc*. **1972**, *94*, 773-778; d) W. Stohrer, R. Hoffmann, *J. Am. Chem. Soc.* **1972***, 94,* 779-786; e) E. Honegger, H. Huber, E. Heilbronner, *J. Am. Chem. Soc*. **1985**, *107,* 7172-7174; f) O. Schafer, M. Allan, G. Szeimies, M. Sanktjohansert, *J. Am. Chem. Soc.* **1992**,*114*,8180-8186; g) M. Messerschmidt, S. Scheins, L. Grubert, M.l Pätzel, G. Szeimies, C. Paulmann, P. Luger, *Angew. Chem. Int. Ed*. **2005**, *44*, 3925 –3928.

[4] B. Braïda, S. Shaik, W. Wu, P. C. Hiberty, *Chem. Eur. J*. **2020**, *26,* 5935-6939.

[5] S. Kozuch, Org. Lett. **2014**, *16*, 4102−4105.

[6] a) I. Fernandez, G. Frenking, *Chem. Eur. J.* **2006**, *12*, 3617 – 3629; b) G. Gayatri, Y. Soujanya, I. Fernández, G. Frenking, G. Narahari Sastry, *J. Phys. Chem. A* **2008**, *112,* 12919–12924. c) Y. Mo, *Org. Lett*. **2006**, *8*(3), 535-538.

[7] Gaussian 09, Revision A.01, M. J. Frisch, G. W. Trucks, H. B. Schlegel, G. E. Scuseria, M. A. Robb, J. R. Cheeseman, G. Scalmani, V. Barone, B. Mennucci, G. A. Petersson, H. Nakatsuji, M. Caricato, X. Li, H. P. Hratchian, A. F. Izmaylov, J. Bloino, G. Zheng, J. L. Sonnenberg, M. Hada, M. Ehara, K. Toyota, R. Fukuda, J. Hasegawa, M. Ishida, T. Nakajima, Y. Honda, O. Kitao, H. Nakai, T. Vreven, J. A. Montgomery, Jr., J. E. Peralta, F. Ogliaro, M. Bearpark, J. J. Heyd, E. Brothers, K. N. Kudin, V. N. Staroverov, R. Kobayashi, J. Normand, K. Raghavachari, A. Rendell, J. C. Burant, S. S. Iyengar, J. Tomasi, M. Cossi, N. Rega, J. M. Millam, M. Klene, J. E. Knox, J. B. Cross, V. Bakken, C. Adamo, J. Jaramillo, R. Gomperts, R. E. Stratmann, O. Yazyev, A. J. Austin, R. Cammi, C. Pomelli, J. W. Ochterski, R. L. Martin, K. Morokuma, V. G. Zakrzewski, G. A. Voth, P. Salvador, J. J. Dannenberg, S. Dapprich, A. D. Daniels, Ö. Farkas, J. B. Foresman, J. V. Ortiz, J. Cioslowski, D. J. Fox, Gaussian, Inc., Wallingford CT, **2009**

[8] Y. Yamaguchi, B. C. Hoffman, J. C. Stephens, H. F. Schaefer, *J. Phys. Chem. A* **1999**, *103*, 38, 7701–7708

[9] K. Exner, P.v. R. Schleyer, *J. Phys. Chem. A* **2001**, *105*, 3407- 3416

[10] a) H. A. Bent, J. Chem. Educ. **1960**, *37* (12)*,* 616–624*;* b) M. J. S. Dewar, H. N. Schmeising, *Tetrahedron* **1959**, *5*, 166-178; c) R. A. Alden, J. Kraut, T. G. Traylor, *J. Am. Chem. Soc.* **1968**, *90*, 74-82; d) S. Osawa, M. Sakai, E. Osawa, *J. Phys. Chem. A* **1997**, *101*, 1378-1383. e) M. G. Brown *Trans. Faraday Soc*., **1959**, *55*, 694-700. f) D. A. Root, C. R. Landis, T. Cleveland, *J. Am. Chem. Soc.* **1993**, *115*, 4201-4209.

[11] M. Tanaka, A. Sekiguchi, *Angew. Chem., Int. Ed.* **2005**, *44*, 5821-5823

[12] a) A. Krapp, F. M. Bickelhaupt, G. Frenking, *Chem. Eur. J*. **2006**, *12*, 9196-9216.

[13] P. Vermeeren, W-J. van Zeist, T. A. Hamlin, C. Fonseca Guerra, F. M. Bickelhaupt**,** *Chem. Eur. J*. **2021** doi.org/10.1002/chem.202004653

[14] F.W. Averill, G. S Painter, *Phys. Rev. B* **1986**, *34(4*) 2088-2095

[15] a) F.M.Bickelhaupt, J. K. Nagle, W.L. Klemm, *J. Phys. Chem. A* **2008**, *112,* 2437-2446; b) P. J. Robinson, A.N. Alexandrova, *J. Phys. Chem. A* **2015**, *119*, 12862−12867. c) P. Chaquin, Y. Canac , C. Lepetit, D. Zargarian, R. Chauvin, *Int. J. Quant. Chem*. **2016**, *116*, 1285-1295; d) P. Chaquin, F. Fuster, F. Volatron, *Int. J. Quant. Chem* **2018**, *118*, 25658-25659

[16] T. Tal, J. Katriel, *Theoret. Chim. Acta* **1977**, *46,* 173-181

[17] a) Y. Yamaguchi, R.B. Remington, J.F. Gaw, H. F. Schaefer III, G. Frenking, *Chem. Phys*. **1994**, 180, 55-70; b) Y. Yamaguchi, R.B. Remington, J.F. Gaw, H. F. Schaefer III, G. Frenking, *J. Chem. Phys*. **1993**, *98* (11), 8749-8760; c) Yamaguchi, B. J. DeLeeuw, C. A. Richards, Jr., H. F. Schaefer III, G. Frenking. *J. Am. Chem. Soc.* **1994***, 116,* 11922-11930.

[18] F. Fuster, P. Chaquin, *Int. J. Quant. Chem.* **2019**,*119 (*20), e25996

[19] R. Laplaza, V. Polo, J. Contreras-Garcia, *J. Phys. Chem. A* **2020**, *124*, 176−184

[20] a) R. D. Bach, O. Dimitrenko, *J. Org. Chem.* **2002**, *67*, 3884-3896; b) R. D. Bach, O. Dimitrenko,, *J. Org. Chem*. **2002**, *67*, 2588-2599; c) S. Grimme*, J. Am. Chem. Soc*. **1996**, *118*, 1529-1534.

[21] J. Blanksby, G. B. Ellison, *Acc. Chem. Res.* **2003**, *36,* 4, 255–263

[22] Y. Mo, Org. Lett. **2006**, *8*(3), 535-538.

[23] a) K. W. Wiberg, *Angew. Chem. Int. Ed. Eng*. **1986**, *25*, 312-322; b) K. W. Wiberg, R.A. Fenoglio, *J. Am. Chem. Soc.* **1968**, *90*, 3395-3397.

[24] D.Cremer, J. Gauss, *J. Am. Chem. Soc*. **1986**, *108*, 7467-7477

[25] R. D. Bach, O. Dimitrenko, *J. Am. Chem. Soc*. **2004** *126*, 4444-4452.